

## Article

# Comparison of Efficacy between Three-Dimensional Printing and Manual-Bending Implants for Inferomedial Orbital Fracture: A Retrospective Study

Jun Hyeok Kim , Chae Rim Lee , Deuk Young Oh, Young-Joon Jun  and Suk-Ho Moon \*

Department of Plastic & Reconstructive Surgery, College of Medicine, The Catholic University of Korea, Seoul 06591, Korea; hyeoggy@catholic.ac.kr (J.H.K.); chaerim.lee@gmail.com (C.R.L.); ehyun@hanmail.net (D.Y.O.); joony@catholic.ac.kr (Y.-J.J.)

\* Correspondence: nasuko@catholic.ac.kr; Tel.: +82-10-9080-3527

**Abstract:** The purpose of reconstruction of an orbital fracture is restoration of normal structure and volume without visible or functional complications. In a previous study, orbital implants were created using three-dimensional (3D) printing technology to restore orbital fractures. In the present study, the authors compared the efficacy of the conventional manual-bending implant and the 3D-printed standardized implant in order to verify the clinical utility of the fabricated 3D printed orbital implant. In this single-center, retrospective study, the authors evaluated medical records and 3D-CT scans of patients with inferomedial orbital fracture. Selected patients were divided into two groups. Group A underwent surgery with the 3D-printed standardized implant, while group B was treated using a manual technique to mold and trim the implant. A total of 32 patients was included in this study, 16 in each group. The volume of the preoperative lesion side was significantly different from that of the normal side or postoperative lesion side within each group. The volume of the postoperative lesion side was not statistically different from that of the normal side in Group A, but this volume was significantly different from that of the normal side in Group B. The 3D-printed standardized implant provides surgical efficacy to restore inferomedial orbital fracture and has superior surgical outcomes to the manual-bending implant.

**Keywords:** inferomedial orbital fracture; 3D printed implants; manual bending



**Citation:** Kim, J.H.; Lee, C.R.; Oh, D.Y.; Jun, Y.-J.; Moon, S.-H. Comparison of Efficacy between Three-Dimensional Printing and Manual-Bending Implants for Inferomedial Orbital Fracture: A Retrospective Study. *Appl. Sci.* **2021**, *11*, 7971. <https://doi.org/10.3390/app11177971>

Academic Editor: Giuliana Muzio

Received: 5 July 2021

Accepted: 26 August 2021

Published: 28 August 2021

**Publisher's Note:** MDPI stays neutral with regard to jurisdictional claims in published maps and institutional affiliations.



**Copyright:** © 2021 by the authors. Licensee MDPI, Basel, Switzerland. This article is an open access article distributed under the terms and conditions of the Creative Commons Attribution (CC BY) license (<https://creativecommons.org/licenses/by/4.0/>).

## 1. Introduction

The purpose of reconstruction of an inferomedial orbital fracture is to restore the normal orbital structure and volume by placing the fractured segment in the premorbid position [1,2]. However, precise restoration of the delicate anatomy of the orbit is challenging [3] and can result in serious and visible enophthalmos, globe dystopia, diplopia, or blindness if sophisticated restoration is not achieved [4–8].

A fractured orbit lacks structural support, and appropriate placement of an implant can be compromised [9,10]. Traditionally, inorganic orbital implants made of titanium, polyethylene, and poly lactic acid have been used [11–15]. Those can be manipulated easily but can lead to above-mentioned complications due to inaccuracy [8] and iatrogenic injury [3]. Recently, the patient-specific implant (PSI) using three-dimensional (3D)-printing technology has been introduced. This implant can be elaborately shaped to restore normal orbital anatomy [2,3,16–25]. However, considering that orbital fracture is a common facial injury, PSI is high-cost, time-consuming, and requiring additional labors for each procedure.

In a previous study, anatomical restoration of an orbital fracture was attempted by creating a suitable implant using 3D printing technology [26]. The orbital implant reproduces the curvature of the inferomedial wall of the orbit using anatomical data from standardized radiologic images of 100 cadavers.

In the present study, the authors compared the efficacy of the conventional manual-bending implant and the 3D-printed standardized implant in clinical practice. The use of a 3D-printed standardized implant was hypothesized to allow more precise molding than a conventional implant. The surgical outcomes were evaluated using computed tomographies to assess the accuracy of implant insertion, the degrees of post-operative enophthalmos and diplopia, and limitation of the globe movement.

## 2. Materials and Methods

In this single-center, retrospective study, we evaluated the medical records and 3D CT scans of patients with inferomedial orbital fracture between May 2017 and October 2019. The Institutional Review Board of The Catholic Medical Center Office of Human Research Protection Program approved our study (IRB approval number: KC21RISI0079). For this type of study, formal consent is not required. The patients were selected according to the following criteria.

The inclusion criteria were:

- a. Diagnosis of unilateral inferomedial orbital fracture with preoperative radiological evaluation including 3D CT
- b. Surgery within two weeks after injury
- c. Postoperative evaluation including clinical outcomes and radiological examination including 3D CT within three months postoperative.

The exclusion criteria were:

- a. Single fracture of the medial wall or floor of the orbit
- b. No preoperative or postoperative 3D CT scans
- c. No postoperative evaluation within three months postoperative
- d. Surrounding combined fracture requiring open reduction and internal fixation such as fracture of the zygomaticomaxillary complex or frontal bone.

Selected patients were divided into two groups. Group A underwent reconstructive surgery with the purchased 3D-printed standardized implant, while group B was treated using a manual technique to mold and trim the 0.8mm polyethylene orbital implant. [Medpor<sup>®</sup>, Stryker Instruments, Kalamazoo, MI, USA].

### 2.1. Fabrication of 3D-Printed Orbital Implant

In the previous study, [26] the data from CT images of 100 adult cadavers were analyzed, and the dimensions of the inferomedial orbital anatomy were reconstituted using a computer-aided design program, 3-matic (version 14.0, Materialize, Leuven, Belgium) [26]. After the implant design was created and simulated based on CT of 10 adult patients, the standardized implant [TnR Mesh (Orbital type), T&R Biofab Co., Ltd., Seoul, Korea] was fabricated at 0.8mm thickness with fused deposition manufacturing 3D printing technology using 3DX printer [T&R Biofab Co., Ltd., Seoul, Korea]. The biocompatible polymer, polycaprolactone (PCL), which is non-toxic, absorbable, absorbent, radiolucent, and semi-rigid with structural stability, was used for this fabrication (Figure 1) [27]. A 100  $\mu$ m thick PCL fibers were dispensed from the steel nozzle of the head at 100 °C and 500 kPa and post-processing was to smooth the edges. It took 3 h to produce one implant, and after production, it was sterilized with a dose of 25 kGy of Gamma irradiation.

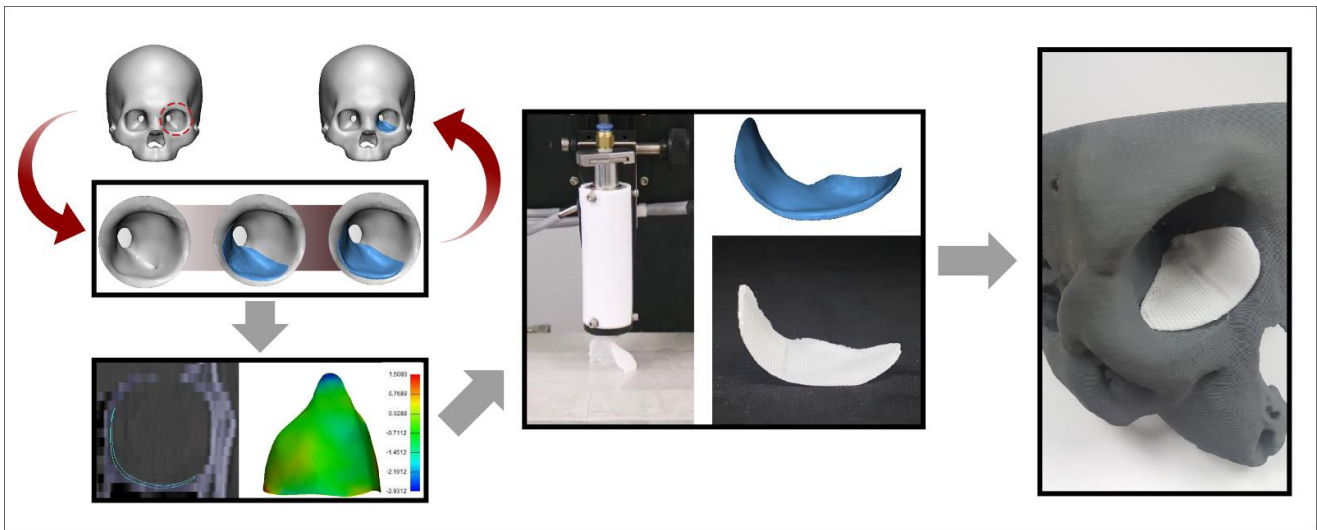


**Figure 1.** Graphical abstract of fabrication of 3D-printed orbital implant.

## 2.2. Clinical Application

Inferomedial orbital fracture diagnoses were confirmed on CT or during surgery. Surgery was performed via a subciliary and transcaruncular approach as previously described [26]. In group A, the standardized 3D-printed implant was applied, while a hand-manipulated orbital implant composed of porous polyethylene was used in group B. To analyze the outcome, the symptoms were evaluated before and after surgery, and orbital volume was measured using CT at 3 days and 2 months after surgery (Figure 2).

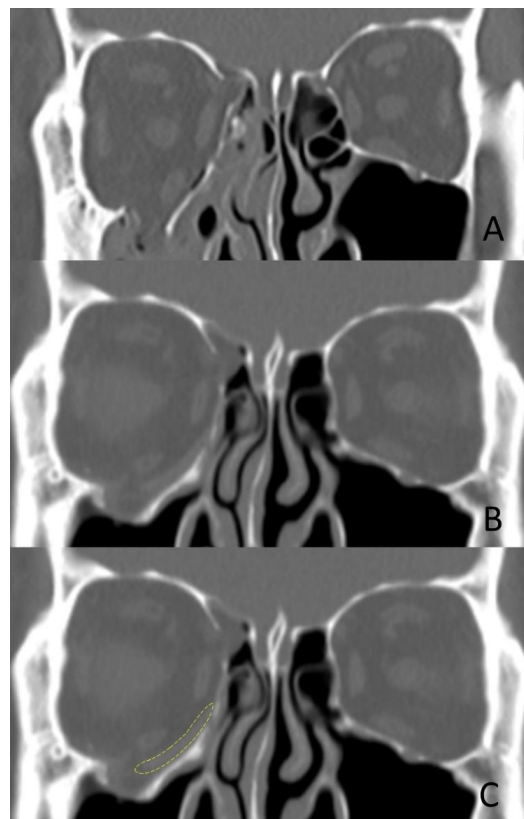


**Figure 2.** CT of a patient with a 3D-printed standardized implant (group (A)) for a right orbital inferomedial fracture. (A) Preoperative CT. (B) At three months postoperative. (C) The implant outline is indicated by a yellow dotted line.

### 2.3. Statistical Analyses

For continuous variables presenting a Gaussian distribution, the mean and SD were used for description, the difference between groups was compared using unpaired t-test, and the repeated-measured one-way ANOVA was used to compare the three measures. For nominal variables, fractions in percentages were calculated, and Fisher's exact test and Chi-square test were used for comparison. A p-value less than 0.05 indicated a statistically significant difference.

### 3. Results

A total of 32 patients was included in this study, 16 in each group. The baseline characteristics and demographic data of the patients are summarized in Table 1. The groups had no differences in age, sex, lesion side, cause of trauma, operational delay, interval of CT, and follow-up period at the outpatient clinic.

**Table 1.** The baseline characteristics and demographic data of the patients.

	Group A	Group B	p Value
Age, year	34.1 ± 16.5	34.6 ± 17.3	0.926
Sex			0.433
Male	13/16 (81.3%)	10/16 (62.5%)	
Female	3/16 (18.8%)	6/16 (37.5%)	
Lesion side			0.716
Rt.	5/16 (31.3%)	7/16 (43.8%)	
Lt.	11/16 (68.8%)	9/16 (56.3%)	
Cause			0.399
Fall down	5/16 (31.3%)	2/16 (12.5%)	
Assault	9/16 (56.3%)	9/16 (56.3%)	
Accidental bump	2/16 (12.5%)	4/16 (25.0%)	
Traffic accident	0/16 (0.0%)	1/16 (6.3%)	
Operation delay, day	7.6 ± 3.1	7.9 ± 2.9	0.773
Interval of CT, day	69.6 ± 49.0	69.5 ± 48.9	0.994
OPD F/U, month	5.1 ± 3.3	5.4 ± 5.5	0.881
Pre-operative symptoms			
Diplopia	2/16 (12.5%)	2/16 (12.5%)	>0.999
Discomfort	3/16 (18.8%)	2/16 (12.5%)	
Exophthalmos	0/16 (0%)	0/16 (0%)	
Post-operative symptoms			
Diplopia	1/16 (6.3%)	1/16 (6.3%)	>0.999
Discomfort	0/16 (0%)	0/16 (0%)	
Exophthalmos	0/16 (0%)	0/16 (0%)	

The mean volumes (cm<sup>3</sup>) of the normal side, preoperative lesion side, and postoperative lesion side of group A were 21.6 ± 2.2, 23.9 ± 2.1, and 21.9 ± 2.1, respectively, and those of group B were 20.6 ± 3.1, 23.1 ± 3.6, and 21.4 ± 3.2. No variable was statistically different between groups (Table 2).

**Table 2. Surgical outcomes: comparison of group A and group B.** (V0: orbital volume of the normal side; Vpre: preoperative orbital volume of the lesion side; Vpost: postoperative orbital volume of the lesion side).

Volume (cm <sup>3</sup> )	Group A	Group B	p-Value
V0	21.6 ± 2.2	20.6 ± 3.1	0.336
Vpre	23.9 ± 2.1	23.1 ± 3.6	0.420
Vpost	21.9 ± 2.1	21.4 ± 3.2	0.628

The volume of the preoperative lesion side was significantly different from the volume of the normal side or postoperative lesion side within each group. The volume of the

postoperative lesion side was not statistically different from the volume of the normal side in Group A, but this volume was significantly different from the volume of the normal side in Group B. (Table 3 and Figure 3)

**Table 3. Surgical outcomes: comparison of variables within each group.** (V0: orbital volume of the normal side; Vpre: preoperative orbital volume of the lesion side; Vpost: postoperative orbital volume of the lesion side). \*\*\*\* *p*-value is significant at the 0.0001 level. \*\*\* *p*-value is significant at the 0.001 level.

Comparisons	<i>p</i> -Value
<b>Group A</b>	
V0 vs. Vpre	<0.0001 ****
V0 vs. Vpost	0.2219
Vpre vs. Vpost	<0.0001 ****
<b>Group B</b>	
V0 vs. Vpre	<0.0001 ****
V0 vs. Vpost	0.0003 ***
Vpre vs. Vpost	0.0004 ***

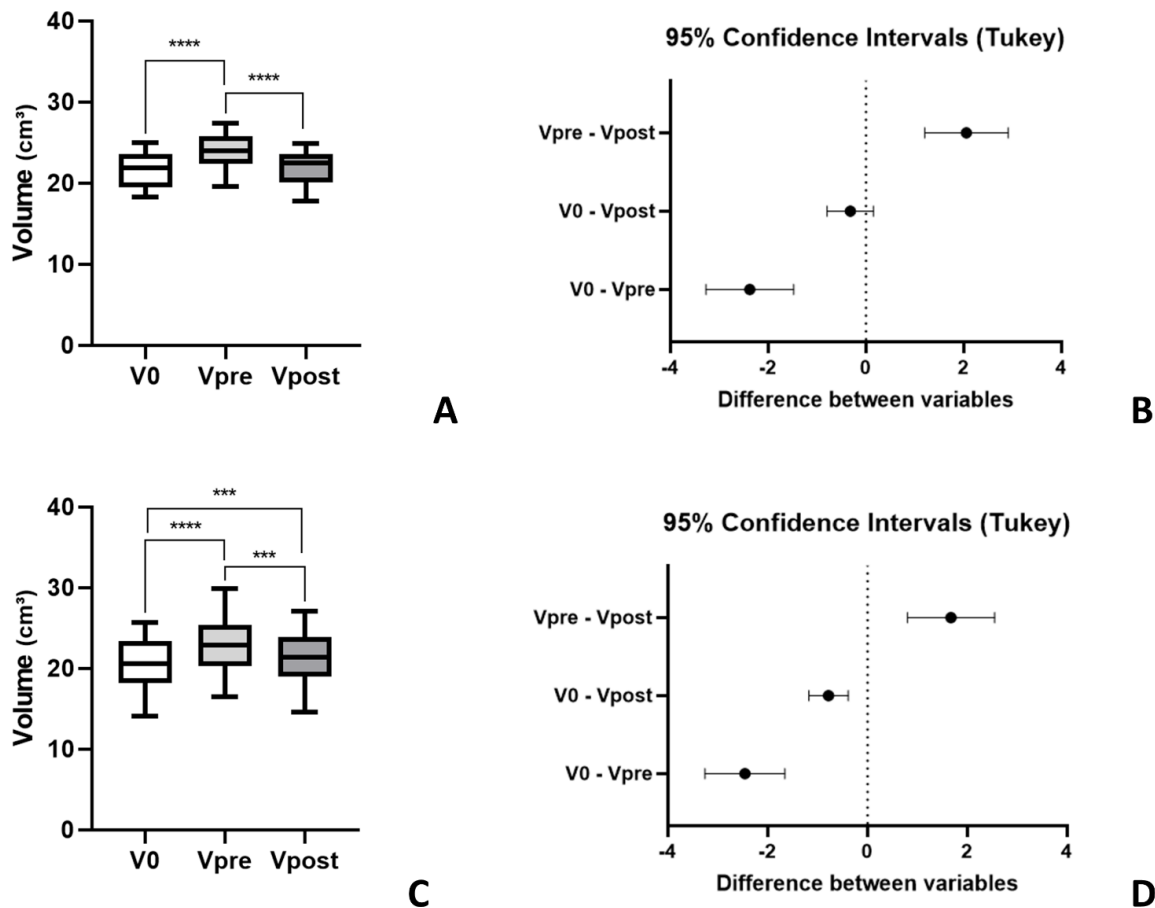


**Figure 3.** Analysis of orbital volume of the normal side and the preoperative and postoperative lesion sides in computed tomography. (V0: orbital volume of the normal side; Vpre: preoperative orbital volume of the lesion side; Vpost: postoperative orbital volume of the lesion side). (A) In group (A), according to repeated measures one-way ANOVA, V0 and Vpost were similar, but differences between V0 and Vpre as between Vpre and Vpost were significant ( $p < 0.05$ ). (B) 95% confidence intervals of group (A) using repeated measures one-way ANOVA. (C) In group (B), according to repeated measures one-way ANOVA, all variables were significantly different ( $p < 0.05$ ). (D) 95% confidence intervals of group B using repeated measures one-way ANOVA.

None of these patients had exophthalmos preoperatively or postoperatively. Three of 16 patients in group A had ocular discomfort before surgery, but the discomfort resolved after surgery. Two of 16 patients in group B had ocular discomfort before surgery, but the discomfort resolved after surgery. Two of 16 patients in group A complained of diplopia before surgery, but only one complained of this after surgery. In group B patients, two of 16 complained of diplopia before surgery, but only one complained of this after surgery (Table 1).

#### 4. Discussion

According to our results, the 3D-printed standardized orbital implant has a more efficient outcome than the conventional manual-bending implant. The volume of the postoperative lesion side was not statistically different from the volume of the normal side in Group A, while those volumes were significantly different in Group B ( $p$ -value < 0.05). Considering that the normal, preoperative, and postoperative side orbital volumes of both groups were not statistically different, as shown in Table 2, the surgical result of group A is superior.

The precise restoration of the fractured orbital structure is important. The restoration requires not only accurate reformation of the orbit but also the appropriate spatial positioning of the globe [16]. However, restoration of the premorbid bony contour [3,16] is challenging and can result in enophthalmos, dystopia, diplopia, and blindness [4–8]. Even a small change in orbital volume can cause significant enophthalmos [28–31].

While the 3D-printed implant is made of PCL, the manual-bending implant is made of polyethylene. PCL, which is approved by the US Food and Drug Administration for use as a medical implant, is a non-toxic, biocompatible, and bio-degradable polymer [27,32]. Polyethylene is a highly stable and flexible material for facial implants and exhibits rapid ingrowth of tissue with collagen deposition and resistance to infection [33]. The most obvious difference between the two materials is that PCL is absorbable and polyethylene is non-absorbable. However, absorbable and non-absorbable implants in orbital wall reconstruction produce similar results in long-term follow-up [34,35]. Therefore, the disparity in results according to the absorbable characteristics of implant materials was excluded in the present study.

Historically, organic autologous implants made of calvarium or cartilage have been introduced in reconstruction of orbital fracture [36]. In addition, inorganic implants including those of titanium, polyethylene, and poly lactic acid have been used [11–15]. Inorganic implants can be manipulated easily but can lead to complications including diplopia, exophthalmos, enophthalmos, or limited ocular movement due to inaccuracy [8]. Additionally possible is iatrogenic injury to the surrounding tissue due to repeated insertion and withdrawal of the implant to obtain the suitable contour [3].

Recently, the PSI using 3D-printing technology has been introduced. This implant can be elaborately shaped to restore normal orbital anatomy at the fracture site [2,3,16–25]. Rapid prototyping (RP) has high applicability because it creates a complex model similar to a normal orbit. RP is used as a template to bend a customized implant made of a polymer such as titanium, [2,3,24,25] because differences between both orbital volumes and contours are clinically minor. [37] PSI is created by computer-aided design and milled by computer-numerical-control from a titanium alloy block [23,38]. However, considering that orbital fracture is a common facial injury, RP and PSI are high-cost and time-consuming. Additional engineers are required to apply the software necessary to produce a customized product for each procedure.

In a previous study, [26] the authors described the creation of a standardized 3D-printed implant. Orbital data obtained by 3D CT at an interval 1 mm from 100 adult cadavers, 50 males with a mean age of 50.4 years (range: 21–60) and 50 females with a mean age of 54.3 years (range: 27–60). The cadavers were limited to those presumed not to cause bone abnormalities due to the cause of death and its complications. In addition, when a metal component by dental treatment was present in the tooth, it was extracted. Then,

orbital data were averaged and used to create 3D-printed implants. The implant design was suitable for a simulation test on 10 adult patients. The 3D-printed implant, which was initially 1.15 mm, now is being fabricated using 0.8-mm-thick polycaprolactone. This is a ready-made standardized implant with precise anatomical contour with no additional cost, time, and labor. Eventually, the standardized implant offers a bridging strategy until the in-housing printing technology of PSI is applicable in the clinical environment.

This study attempted to achieve accurate restoration of the orbital cavity using a standardized 3D printing implant. This might be a satisfactory bridging strategy until technological advancement allows in-house printing of PSI.

The limitations of the present study are that it has a retrospective design, not a randomized controlled trial. And the exact measurement point of orbital volume cannot be defined. Additionally, the number of participating patients was small.

## 5. Conclusions

The 3D-printed standardized implant provides surgical efficacy to restore inferomedial orbital fracture. It presents superior surgical outcomes to the manual-bending implant and offers a pass-through strategy until the in-housing printing technology of PSI is applicable in the common clinical environment.

**Author Contributions:** Conceptualization, J.H.K. and S.-H.M.; methodology, S.-H.M.; software, C.R.L.; validation, D.Y.O. and Y.-J.J.; formal analysis, J.H.K.; investigation, C.R.L.; resources, J.H.K.; data curation, C.R.L.; writing—original draft preparation, J.H.K.; writing—review and editing, S.-H.M.; visualization, J.H.K.; supervision, D.Y.O.; project administration, S.-H.M.; funding acquisition, S.-H.M. All authors have read and agreed to the published version of the manuscript.

**Funding:** This work was supported by the National Research Foundation of Korea (NRF) grant funded by the Korea government (MSIT) (2017M3A9E2060428).

**Institutional Review Board Statement:** Our study was approved by the Institutional Review Board of The Catholic Medical Center Office of Human Research Protection Program. (IRB approval number: KC21RISI0079).

**Informed Consent Statement:** The requirement for informed consent was waived due to the retrospective nature of the study.

**Data Availability Statement:** Data available on request due to restrictions e.g., privacy or ethical. The data presented in this study are available on request from the corresponding author. The data are not publicly available because it contains processed patient information.

**Conflicts of Interest:** The authors declare no conflict of interest.

## References

1. Hammer, B.; Prein, J. Correction of post-traumatic orbital deformities: Operative techniques and review of 26 patients. *J. Cranio-Maxillofac. Surg.* **1995**, *23*, 81–90. [[CrossRef](#)]
2. Oh, T.S.; Jeong, W.S.; Chang, T.J.; Koh, K.S.; Choi, J.W. Customized orbital wall reconstruction using three-dimensionally printed rapid prototype model in patients with orbital wall fracture. *J. Craniofac. Surg.* **2016**, *27*, 2020–2024. [[CrossRef](#)]
3. Kim, Y.C.; Jeong, W.S.; Park, T.K.; Choi, J.W.; Koh, K.S.; Oh, T.S. The accuracy of patient specific implant prebent with 3D-printed rapid prototype model for orbital wall reconstruction. *J. Cranio-Maxillofac. Surg.* **2017**, *45*, 28–36. [[CrossRef](#)]
4. Goldberg, R.A.; Shorr, N.; Cohen, M.S. The medical orbital strut in the prevention of postdecompression dystopia in dysthyroid ophthalmopathy. *Ophthalmic Plast. Reconstr. Surg.* **1992**, *8*, 32–34. [[CrossRef](#)] [[PubMed](#)]
5. Jordan, D.R.; Anderson, R.L. Orbital decompression. *Ophthalmic Plast. Reconstr. Surg.* **2000**, *16*, 167–168. [[CrossRef](#)] [[PubMed](#)]
6. Stathopoulos, P.; Ameerally, P. Reconstructing a traumatic empty orbit: Principles, difficulties of treatment, and literature review. *Journal of oral and maxillofacial surgery. Off. J. Am. Assoc. Oral Maxillofac. Surg.* **2018**, *76*, 1952–e1. [[CrossRef](#)]
7. Wright, E.D.; Davidson, J.; Codere, F.; Desrosiers, M. Endoscopic orbital decompression with preservation of an inferomedial bony strut: Minimization of postoperative diplopia. *J. Otolaryngol.* **1999**, *28*, 252–256. [[PubMed](#)]
8. Shin, J.W.; Lim, J.S.; Yoo, G.; Byeon, J.H. An analysis of pure blowout fractures and associated ocular symptoms. *J. Craniofac. Surg.* **2013**, *24*, 703–707. [[CrossRef](#)]
9. Hur, S.W.; Kim, S.E.; Chung, K.J.; Lee, J.H.; Kim, T.G.; Kim, Y.H. Combined orbital fractures: Surgical strategy of sequential repair. *Arch. Plast. Surg.* **2015**, *42*, 424–430. [[CrossRef](#)]

10. Su, G.W.; Harris, G.J. Combined inferior and medial surgical approaches and overlapping thin implants for orbital floor and medial wall fractures. *Ophthalmic. Plast. Reconstr. Surg.* **2006**, *22*, 420–423. [[CrossRef](#)]
11. Cordewener, F.W.; Bos, R.R.; Rozema, F.R.; Houtman, W.A. Poly(L-lactide) implants for repair of human orbital floor defects: Clinical and magnetic resonance imaging evaluation of long-term results. *J. Oral Maxillofac. Surg.* **1996**, *54*, 9–13. [[CrossRef](#)]
12. Dietz, A.; Ziegler, C.M.; Dacho, A.; Althof, F.; Conradt, C.; Kolling, G.; von Boehmer, H.; Steffen, H. Effectiveness of a new perforated 0.15 mm poly-p-dioxanon-foil versus titanium-dynamic mesh in reconstruction of the orbital floor. *J. Maxillofac. Surg.* **2001**, *29*, 82–88. [[CrossRef](#)] [[PubMed](#)]
13. Xu, J.J.; Teng, L.; Jin, X.L.; Ji, Y.; Lu, J.J.; Zhang, B. Porous polyethylene implants in orbital blow-out fractures and enophthalmos reconstruction. *J. Craniofac. Surg.* **2009**, *20*, 918–920. [[PubMed](#)]
14. Ono, I.; Gunji, H.; Suda, K.; Kaneko, F.; Yago, K. Orbital reconstruction with hydroxyapatite ceramic implants. *Scand. J. Plast. Reconstr. Surg. Hand Surg.* **1994**, *28*, 193–198. [[CrossRef](#)] [[PubMed](#)]
15. Tuncer, S.; Yavuzer, R.; Kandal, S.; Demir, Y.H.; Ozmen, S.; Latifoglu, O.; Atabay, K. Reconstruction of traumatic orbital floor fractures with resorbable mesh plate. *J. Craniofac. Surg.* **2007**, *18*, 598–605. [[CrossRef](#)]
16. Stoor, P.; Suomalainen, A.; Lindqvist, C.; Mesimaki, K.; Danielsson, D.; Westermarck, A.; Kontio, R.K. Rapid prototyped patient specific implants for reconstruction of orbital wall defects. *J. Cranio-Maxillofac. Surg.* **2014**, *42*, 1644–1649. [[CrossRef](#)]
17. Kozakiewicz, M. Computer-aided orbital wall defects treatment by individual design ultrahigh molecular weight polyethylene implants. *J. Cranio-Maxillofac. Surg.* **2014**, *42*, 283–289. [[CrossRef](#)]
18. Lieger, O.; Richards, R.; Liu, M.; Lloyd, T. Computer-assisted design and manufacture of implants in the late reconstruction of extensive orbital fractures. *Arch. Facial Plast. Surg.* **2010**, *12*, 186–191. [[CrossRef](#)]
19. Metzger, M.C.; Schön, R.; Weyer, N.; Rafii, A.; Gellrich, N.C.; Schmelzeisen, R.; Strong, B.E. Anatomical 3-dimensional pre-bent titanium implant for orbital floor fractures. *Ophthalmology* **2006**, *113*, 1863–1868. [[CrossRef](#)]
20. Cha, J.H.; Moon, M.H.; Lee, Y.H.; Koh, I.C.; Kim, K.N.; Kim, C.G.; Kim, H. Correlation between the 2-dimensional extent of orbital defects and the 3-dimensional volume of herniated orbital content in patients with isolated orbital wall fractures. *Arch. Plast. Surg.* **2017**, *44*, 26–33. [[CrossRef](#)]
21. Hassfeld, S.; Muhling, J. Computer assisted oral and maxillofacial surgery—A review and an assessment of technology. *International J. Oral Maxillofac. Surg.* **2001**, *30*, 2–13. [[CrossRef](#)]
22. Vignesh, U.; Mehrotra, D.; Anand, V.; Howlader, D. Three dimensional reconstruction of late post traumatic orbital wall defects by customized implants using CAD-CAM, 3D stereolithographic models: A case report. *J. Oral Biol. Craniofacial Res.* **2017**, *7*, 212–218. [[CrossRef](#)]
23. Gander, T.; Essig, H.; Metzler, P.; Lindhorst, D.; Dubois, L.; Rücker, M.; Schumann, P. Patient Specific Implants (PSI) in reconstruction of orbital floor and wall fractures. *J. Cranio-Maxillofac. Surg.* **2015**, *43*, 126–130. [[CrossRef](#)] [[PubMed](#)]
24. Vehmeijer, M.; van Eijnatten, M.; Liberton, N.; Wolff, J. A novel method of orbital floor reconstruction using virtual planning, 3-dimensional printing, and autologous bone. *J. Oral Maxillofac. Surg.* **2016**, *74*, 1608–1612. [[CrossRef](#)] [[PubMed](#)]
25. Kronig, S.A.J.; Van Der Mooren, R.J.G.; Strabbing, E.M.; Stam, L.H.M.; Tan, J.A.S.L.; De Jongh, E.; van der Wal, K.G.H.; Paridaens, D.; Koudstaal, M.J. Pure orbital blowout fractures reconstructed with autogenous bone grafts: Functional and aesthetic outcomes. *International J. Oral Maxillofac. Surg.* **2016**, *45*, 507–512. [[CrossRef](#)] [[PubMed](#)]
26. Kim, J.H.; Lee, I.G.; Lee, J.S.; Oh, D.Y.; Jun, Y.J.; Rhie, J.W.; Shim, J.H.; Moon, S.H. Restoration of the inferomedial orbital strut using a standardized three-dimensional printing implant. *J. Anat.* **2020**, *236*, 923–930. [[CrossRef](#)]
27. Teo, L.; Teoh, S.H.; Liu, Y.; Lim, L.; Tan, B.; Schantz, J.T.; Seah, L.L. A novel bioresorbable implant for repair of orbital floor fractures. *Orbit* **2015**, *34*, 192–200. [[CrossRef](#)]
28. Parsons, G.S.; Mathog, R.H. Orbital wall and volume relationships. *Arch. Otolaryngol. Head Neck Surg.* **1988**, *114*, 743–747. [[CrossRef](#)]
29. Jin, H.R.; Shin, S.O.; Choo, M.J.; Choi, Y.S. Relationship between the extent of fracture and the degree of enophthalmos in isolated blowout fractures of the medial orbital wall. *J. Oral Maxillofac. Surg.* **2000**, *58*, 617–620. [[CrossRef](#)]
30. Ploder, O.; Klug, C.; Voracek, M.; Burggasser, G.; Czerny, C. Evaluation of computer-based area and volume measurement from coronal computed tomography scans in isolated blowout fractures of the orbital floor. *J. Oral Maxillofac. Surg.* **2002**, *60*, 1267–1272. [[CrossRef](#)]
31. Zhang, Z.; Zhang, Y.; He, Y.; An, J.; Zwahlen, R.A. Correlation between volume of herniated orbital contents and the amount of enophthalmos in orbital floor and wall fractures. *J. Oral Maxillofac. Surg.* **2012**, *70*, 68–73. [[CrossRef](#)] [[PubMed](#)]
32. Lee, S.-H.; Lee, J.H.; Cho, Y.-S. Analysis of degradation rate for dimensionless surface area of well-interconnected PCL scaffold via in-vitro accelerated degradation experiment. *Tissue Eng. Regen. Med.* **2014**, *11*, 446–452. [[CrossRef](#)]
33. Wellisz, T. Clinical experience with the Medpor porous polyethylene implant. *Aesthetic Plast. Surg.* **1993**, *17*, 339–344. [[CrossRef](#)]
34. Baek, W.I.; Kim, H.K.; Kim, W.S.; Bae, T.H. Comparison of absorbable mesh plate versus titanium-dynamic mesh plate in reconstruction of blow-out fracture: An analysis of long-term outcomes. *Arch. Plast. Surg.* **2014**, *41*, 355–361. [[CrossRef](#)]
35. Hwang, K.; Kim, D.H. Comparison of the supporting strength of a poly-L-lactic acid sheet and porous polyethylene (Medpor) for the reconstruction of orbital floor fractures. *J. Craniofac. Surg.* **2010**, *21*, 847–853. [[CrossRef](#)]
36. Strong, E.B. Orbital fractures: Pathophysiology and implant materials for orbital reconstruction. *Facial Plast. Surg.* **2014**, *30*, 509–517. [[CrossRef](#)]

- 
37. Jansen, J.; Dubois, L.; Schreurs, R.; Gooris, P.J.; Maal, T.J.; Beenen, L.F.; Becking, A.G. Should virtual mirroring be used in the preoperative planning of an orbital reconstruction? *J. Oral Maxillofac. Surg.* **2018**, *76*, 380–387. [[CrossRef](#)]
  38. Karkkainen, M.; Wilkman, T.; Mesimaki, K.; Snall, J. Primary reconstruction of orbital fractures using patient-specific titanium milled implants: The Helsinki protocol. *Br. J. Oral Maxillofac. Surg.* **2018**, *56*, 791–796. [[CrossRef](#)] [[PubMed](#)]